

---

# On Consistency in Graph Neural Network Interpretation

---

**Tianxiang Zhao, Dongsheng Luo, Xiang Zhang, Suhang Wang**

College of Information Sciences and Technology

The Pennsylvania State University

State College, PA 16801

tkz5084, dul262, xzz89, szw494@psu.edu

## Abstract

Uncovering rationales behind predictions of graph neural networks (GNNs) has received increasing attention over recent years. Instance-level GNN explanation aims to discover critical input elements, like nodes or edges, that the target GNN relies upon for making predictions. These identified sub-structures can provide interpretations of GNN’s behavior. Though various algorithms are proposed, most of them formalize this task by searching the minimal subgraph which can preserve original predictions. An inductive bias is deep-rooted in this framework: the same output cannot guarantee that two inputs are processed under the same rationale. Consequently, they have the danger of providing spurious explanations and fail to provide consistent explanations. Applying them to explain weakly-performed GNNs would further amplify these issues. To address the issues, we propose to obtain more faithful and consistent explanations of GNNs. After a close examination on predictions of GNNs from the causality perspective, we attribute spurious explanations to two typical reasons: confounding effect of latent variables like distribution shift, and causal factors distinct from the original input. Motivated by the observation that both confounding effects and diverse causal rationales are encoded in internal representations, we propose a simple yet effective countermeasure by aligning embeddings. This new objective can be incorporated into existing GNN explanation algorithms with no effort. We implement both a simplified version based on absolute distance and a distribution-aware version based on anchors. Experiments on 5 datasets validate its effectiveness, and theoretical analysis shows that it is in effect optimizing a more faithful explanation objective in design, which further justifies the proposed approach.

## 1 Introduction

With the growing interest in learning from graph-structured data [17, 39], graph neural networks (GNNs) are receiving more and more attention over the years. In general, GNNs adopt message-passing to recursively propagate and fuse messages on the graph, and have achieved state-of-the-art performance for many graph learning tasks [14, 12, 32, 37]. Despite their success, as with other neural networks, GNNs lack interpretability. Understanding GNNs’ predictions is very important. First, it enhances practitioners’ trust in the GNN model by enriching their understanding of the network characteristics. Second, it increases the models’ transparency to enable trusted applications in decision-critical fields sensitive to fairness, privacy and safety challenges, such as healthcare and drug discovery [20].

Particularly, we focus on post-hoc instance-level explanations. Given a trained GNN and an input graph, this task seeks to discover the sub-structures that can explain the prediction behavior of the

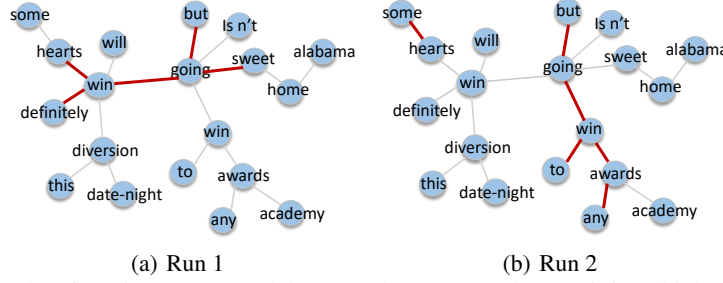


Figure 1: Example of testing GNNExplainer on dataset Graph-SST5, in which two random run produce different explanations.

GNN model. Many solutions have been proposed [33, 13, 27]. For example, Ying et al. [33] learn an importance matrix on nodes and edges via perturbation. The identified minimal sub-structures that preserve original prediction are taken as the explanation. Extending this idea, Luo et al. [16] trains a graph generator to utilize global information in explanation and enable faster inference in the inductive setting. Yuan et al. [36] constraints explanations as connected sub-graphs and conducts Monte Carlo tree search. Despite differences in algorithm design, these methods can be summarized in a label preserving framework, i.e., candidate explanation is formed as a masked version of the original graph and is identified as the minimal discriminative substructure that preserves the predicted label.

However, with the complexity in topology and the combinatory number of candidate sub-structures, existing label preserving methods are insufficient for faithful and consistent explanation of GNNs. They are prone to highlighting spurious correlations as valid explanations. A failure case is shown in Fig. 1, where a GNN is trained on Graph-SST5 [35] for sentiment classification. Each node represents a word and edges denote syntactic dependencies. Each graph is labeled based on sentiment of the sentence. In this figure, the sentence “Sweet home alabama isn’t going to win any academy awards, but this date-night diversion will definitely win some hearts” is labeled *positive* and the real explanation should be “definitely win some hearts”. However, GNNExplainer [33] could mistakenly mask out “isn’t” and identify “win academy awards” to be the explanation. This problem of spurious explanation is largely neglected by existing methods. In addition, across running with different random seeds, they have the danger of generating different explanations (see Fig. 1), breaking the criteria of **consistency**, i.e., the explanation method should be deterministic and consistent to the same input for different runs [18].

With close inspections, we find that the arise of this phenomenon can be understood via examining inference of target GNNs from the causality perspective. Existing explanation methods may lead to spurious explanations either as a result of different causal factors or due to confounding effect of distribution shifts (identified subgraphs may be O.O.D). These failure cases originate from one particular inductive bias: assuming that predicted labels are sufficiently indicative towards finding critical input components, which is rooted in their optimization objective. Based on these findings, we propose a new objective that encourages alignment of embeddings of raw graph and identified subgraph in search of explanations. Considering the inference of GNNs, both confounding effects and distinct causal relationships can be reflected in internal representation space. Therefore, this new objective can provide more genuine explanations of the underlying prediction rationale. Concretely, we propose two strategies based on absolute distance and relative distributions respectively, to achieve embedding alignment. Both variants are flexible to be incorporated into various existing GNN explanation methods. Despite being intuitive and easy-to-apply, further analysis shows that the proposed method is in fact optimizing a new explanation framework, which is more faithful in design. Extensive experiments on real-world and synthetic datasets further show that our framework provides more faithful and consistent explanations, and can benefit various GNN explainers.

## 2 Preliminary

### 2.1 Problem Definition

We use  $\mathcal{G} = \{\mathcal{V}, \mathcal{E}; \mathbf{F}, \mathbf{A}\}$  to denote a graph, where  $\mathcal{V} = \{v_1, \dots, v_n\}$  is a set of  $n$  nodes and  $\mathcal{E} \in \mathcal{V} \times \mathcal{V}$  is the set of edges. Nodes are accompanied by an attribute matrix  $\mathbf{F} \in \mathbb{R}^{n \times d}$ , and

$\mathbf{F}[i,:] \in \mathbb{R}^{1 \times d}$  is the  $d$ -dimensional node attributes of node  $v_i$ .  $\mathcal{E}$  is described by an adjacency matrix  $\mathbf{A} \in \mathbb{R}^{n \times n}$ .  $A_{ij} = 1$  if there is an edge between node  $v_i$  and  $v_j$ ; otherwise,  $A_{ij} = 0$ . For *graph classification*, each graph  $\mathcal{G}_i$  has a label  $Y_i \in \mathcal{C}$ , and a GNN model  $f$  is trained to map  $\mathcal{G}$  to its class, i.e.,  $f : \{\mathbf{F}, \mathbf{A}\} \mapsto \{1, 2, \dots, C\}$ . Similarly, for *node classification*, each graph  $\mathcal{G}_i$  denote a  $K$ -hop subgraph centered at node  $v_i$  and a GNN model  $f$  is trained to predict the label of  $v_i$  based on node representation of  $v_i$  learned from  $\mathcal{G}_i$ . The purpose of explanation is to find a subgraph  $\mathcal{G}'$ , marked with binary importance mask  $\mathbf{M}_A \in [0, 1]^{n \times n}$  on adjacency matrix and  $\mathbf{M}_F \in [0, 1]^{n \times d}$  on node attributes, e.g.,  $\mathcal{G}' = \{\mathbf{A} \odot \mathbf{M}_A; \mathbf{X} \odot \mathbf{M}_F\}$ , where  $\odot$  denotes element-wise multiplication. These two masks highlight components of  $\mathcal{G}$  that are important for  $f$  to predict its label.

## 2.2 MMI-based Explanation Framework

Many approaches have been designed for instance-level post-hoc GNN explanation. Due to the discreteness of edge existence and non-grid graph structures, most works [33, 16] apply a perturbation-based strategy for evaluating and searching explanations. Typically, they can be summarized as Maximization of Mutual Information (MMI) between predicted label  $\hat{Y}$  and explanation  $\mathcal{G}'$ , i.e.,

$$\begin{aligned} & \min_{\mathcal{G}'} -I(\hat{Y}, \mathcal{G}'), \\ \text{s.t. } & \mathcal{G}' \sim \mathcal{P}(\mathcal{G}, \mathbf{M}_A, \mathbf{M}_F), \quad \mathcal{R}(\mathbf{M}_F, \mathbf{M}_A) \leq c \end{aligned} \quad (1)$$

where  $I()$  represents mutual information and  $\mathcal{P}$  denotes the perturbations on original input with importance masks  $\{\mathbf{M}_F, \mathbf{M}_A\}$ . For example, using  $\{\hat{\mathbf{A}}, \hat{\mathbf{F}}\}$  to represent perturbed  $\{\mathbf{A}, \mathbf{F}\}$ ,  $\hat{\mathbf{A}} = \mathbf{A} \odot \mathbf{M}_A$  and  $\hat{\mathbf{F}} = \mathbf{Z} + (\mathbf{F} - \mathbf{Z}) \odot \mathbf{M}_F$  in GNNExplainer [33], where  $\mathbf{Z}$  is sampled from marginal distribution of node attributes  $\mathbf{F}$ .  $\mathcal{R}$  denotes regularization terms on the explanation, imposing prior knowledge into the searching process, like constraints on budgets or connectivity distributions [16]. Mutual information  $I(\hat{Y}, \mathcal{G}')$  quantifies consistency between original predictions  $\hat{Y} = f(\mathcal{G})$  and prediction of candidate explanation  $f(\mathcal{G}')$ , which promotes the positiveness of found explanation  $\mathcal{G}'$ . Since mutual information measures the predictive power of  $\mathcal{G}'$  on  $\hat{Y}$ , this framework essentially tries to find a subgraph that can best predict the original output  $\hat{Y}$ . During training, a relaxed version [33] is often adopted as:

$$\begin{aligned} & \min_{\mathcal{G}'} H_C(\hat{Y}, P(\hat{Y}' \mid \mathcal{G}')), \\ \text{s.t. } & \mathcal{G}' \sim \mathcal{P}(\mathcal{G}, \mathbf{M}_A, \mathbf{M}_F), \quad \mathcal{R}(\mathbf{M}_F, \mathbf{M}_A) \leq c \end{aligned} \quad (2)$$

where  $H_C$  denotes cross-entropy. Targeting on this objective, existing algorithms mainly differ from each other in terms of searching strategies.

Different aspects regarding quality of explanations can be evaluated [18]. Among them, two most important criteria are **faithfulness** and **consistency**. Faithfulness measures the descriptive accuracy of explanations, indicating how truthful they are compared to behaviors of target model. Consistency considers explanation invariance, which checks that identical input should have identical explanations. However, as the example in Fig. 1, existing MMI-based framework is sub-optimal regarding these requirements. Cause of this problem is rooted in learning objective, which uses prediction alone as the guidance in search of explanations. A detailed analysis will be provided in the next section.

## 3 Analyze Spurious Explanations

With “spurious explanations”, we refer to those explanations lying outside the genuine rationale of prediction on  $\mathcal{G}$ , making the usage of  $\mathcal{G}'$  as explanations anecdotal, yielding erroneous explanations. As shown in Fig. 1, despite rapid developments in explaining GNNs, the problem w.r.t faithfulness and consistency of found explanations remains. To get a deeper understanding of reasons behind this problem, we can examine behavior of the target GNN model from the causality perspective, as Structural Equation Model (SEM) in Fig. 2(a). variable  $C$  denotes discriminative causal factors and variable  $S$  represents confounding environment factors: (1)  $\mathcal{G} \rightarrow C \rightarrow Y$  presents the inference that relies on critical patterns  $C$  extracted from input graph that are informative and discriminative. (2) In  $\mathcal{G} \leftarrow S \rightarrow Y$ ,  $S$  denotes confounding factors, such as depicting the overall distribution of graphs. It is causally related to both the appearance of input graphs and prediction of target GNN models. Masked version of  $\mathcal{G}$  could create out-of-distribution (OOD) examples, resulting in spurious causality

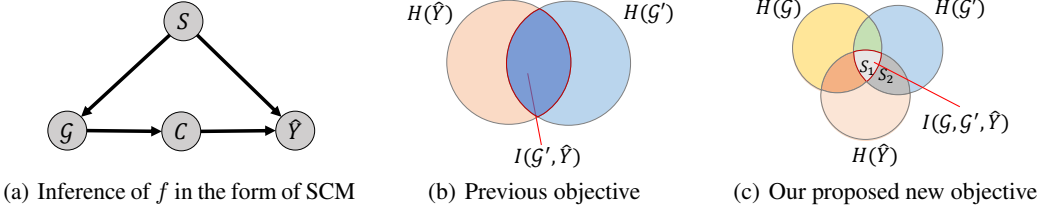


Figure 2: Analysis on spurious explanations. Inference of  $f$  is depicted as a causal graph in (a), with  $S$  for confounding factors and  $C$  for causal variables. Previous objective (b) over-relies on preserving predicted labels, and cannot guarantee faithful explanations compared to ours (c).

to prediction outputs. For example in the chemical domain, removing edges (bonds) or nodes (atoms) may obtain invalid molecular graphs that never appear during training.

Fig. 2(a) provides us with a tool to analyze  $f$ ’s behaviors. From obtained causal structures, we can observe that spurious explanations may arise as a result of failure in recovering original causal rationale.  $\mathcal{G}'$  learned from Eq. 1 may preserve prediction  $\hat{Y}$  due to confounding effect of distribution shift or different causal variables  $C$  compared to original  $\mathcal{G}$ . Weakly-trained GNN  $f(\cdot)$  would further amplify this problem as the prediction is unreliable.

To further understand the issue, we can build the correspondence from SEM in Fig. 2(a) to inference process of GNN model  $f$ . Decomposing GNN  $f()$  as a feature extractor  $f_1()$  and a classifier  $f_2()$ , its inference can be summarized as two steps: (1) Representation learning step with  $f_1()$ , which takes  $\mathcal{G}$  as input and produces its embedding in the representation space  $E_C$ ; (2) Classification step with  $f_2()$ , which predicts output labels on input’s embedding. Connecting to SEM in Fig. 2(a), we can find that:

- Causal path  $\mathcal{G} \rightarrow C \rightarrow Y$  lies behind the inference process with representation space  $E_C$  to encode critical variables  $C$ ;
- Confounding effect of distribution shift  $S$  works on the inference process via influencing distribution of graph embedding in  $E_C$ . When masked input  $\mathcal{G}'$  is OOD, its embedding would fail to reflect its discriminative features and deviate from real distributions, hence mislead the classification step on it.

## 4 Methodology

Based on previous discussions, we propose to study a novel task in this work: improving faithfulness and consistency of GNN explanations and overcoming the inductive bias of relying upon prediction outputs. A simple countermeasure is proposed by aligning node and graph embeddings of  $\mathcal{G}$  and  $\mathcal{G}'$ , to promote that  $\mathcal{G}'$  is seen and processed uniformly as original  $\mathcal{G}$  by  $f$ .

### 4.1 Alleviation of Spurious Explanations

Instance-level post-hoc explanation dedicates to finding discriminative substructures the target model  $f$  depends upon. Traditional learning objective in Eq. 2 can identify minimal predictive parts of input, however, it is dangerous to directly take them as explanations in the graph domain. Due to diversity in graph topology and combinatorial nature of sub-graphs, multiple distinct substructures could be identified leading to the same prediction. A clearer illustration is provided in Fig. 2(a), which shows that predicted labels are influenced by various causal factors as well as confounding effects from distribution shift.

Following analysis in Section 3, we propose to take an alternative approach by looking into internal embeddings learned by  $f$ . Causal variables  $C$  are encoded in representation space extracted by  $f$ , and out-of-distribution effects can also be reflected by analyzing embedding distributions. Motivated by these observations, one assumption can be safely made: *if two graphs are mapped to embeddings near each other by a GNN layer, then they are seen as similar by it and would be processed similarly by following layers*. With this assumption, a proxy task can be designed by aligning internal graph embeddings between  $\mathcal{G}'$  and  $\mathcal{G}$  inside target model  $f$ .

Let  $\mathbf{h}_v^l$  be the representation of node  $v$  at the  $l$ -th GNN layer with  $\mathbf{h}_v^0 = \mathbf{F}[i, :]$ . Generally, the inference process inside GNN layers can be summarized as a message-passing framework:

$$\mathbf{m}_v^{l+1} = \sum_{u \in \mathcal{N}(v)} M_l(\mathbf{h}_v^l, \mathbf{h}_u^l, A_{v,u}), \quad \mathbf{h}_v^{l+1} = U_l(\mathbf{h}_v^l, \mathbf{m}_v^{l+1}), \quad (3)$$

where  $M_l$  and  $U_l$  are the message function and update function at  $l$ -th layer, respectively.  $\mathcal{N}_v$  are the set of neighbors of node  $v$ . Without loss of generality, the graph pooling layer can also be presented as  $\mathbf{h}_{v'}^{l+1} = \sum_{v \in \mathcal{V}} P_{v,v'} \cdot \mathbf{h}_v^l$ , where  $P_{v,v'}$  denotes the mapping weight from node  $v$  in layer  $l$  to node  $v'$  in layer  $l+1$  inside the myriad of GNN. In this work, we focus on aligning updated embedding  $\mathbf{h}_v^{l+1}$  at each layer, which contains both node and local neighborhood information.

## 4.2 Embedding Alignment

To achieve alignment in embedding space, there are several important design considerations: (1) Intermediate embeddings are usually high-dimensional, could suffer from the curse of dimensionality [26]; (2) Each dimension of embeddings may carry different importance, and it could be sub-optimal treating them as equal; (3) Measurement of alignment need to be carefully selected, which should be both easy-to-compute and correlate well to distance on distribution manifold. Different answers to these considerations motivate the design of different alignment strategies. In this work, we propose two strategies: a simplified version based on absolute distance and local importance estimations, and an anchor-based version achieving alignment in the distribution-aware manner.

**Absolute Distance-based** The first strategy achieves alignment based on absolute distance in embedding space. At the  $l$ -th layer, we denote input representations of node  $v$  as  $\mathbf{h}_v^l$ . Without graph pooling, the alignment can be written as:

$$\mathcal{L}_{align}(f(\mathcal{G}), f(\mathcal{G}')) = \sum_l \sum_{v \in \mathcal{V}} \|\mathbf{h}_v^l - \hat{\mathbf{h}}_v^l\|_2^2 \quad (4)$$

For layers with graph pooling, as graph structure is changed, we conduct alignment on global graph representation calculated with  $\sum_{v \in \mathcal{V}'} \mathbf{h}_v^{l+1} / |\mathcal{V}'|$ , where  $\mathcal{V}'$  denotes node set after pooling. In this strategy, alignment is conducted based on absolute distance on graph embeddings. Note that some extensions can be made. For example, gradients can be used as the 1st-order estimation on importance of each dimension to conduct weighted alignment on  $\frac{\partial f(\mathcal{G})}{\partial \mathbf{h}_v^l} \odot \mathbf{h}_v^l$ . For simplicity, we stick to absolute distance in this strategy and leave the exploration of other extensions as future works.

**Global Anchor-based** Instead of taking all input examples as independent, the second strategy can identify explanatory substructures and preserve their alignment with original graphs in a distribution-aware manner. The basic idea is to utilize other graphs to obtain a global view on distribution density of embeddings, providing a better measurement on alignment. Concretely, we obtain representative node/graph embeddings as anchors, and use distances to these anchors as the distribution-aware graph representations. Then, alignment is evaluated by comparing obtained representation of graph pairs. The detailed steps are: (1) Using graphs  $\{\mathcal{G}_i\}_{i=1}^m$  from the same dataset, a set of node embeddings can be obtained as  $\{\{\mathbf{h}_{v,i}^l\}_{v \in \mathcal{V}_i'}\}_{i=1}^m$  for each layer  $l$ , where  $\mathbf{h}_{v,i}^l$  denotes embedding of node  $v$  in graph  $\mathcal{G}_i$ . For node-level tasks, we set  $\mathcal{V}_i'$  to contain only the center node of graph  $\mathcal{G}_i$ . For graph-level tasks,  $\mathcal{V}_i'$  contains nodes set after graph pooling layer, and we process them following  $\{\sum_{v \in \mathcal{V}_i'} \mathbf{h}_{v,i}^{l+1} / |\mathcal{V}_i'|\}_{i=1}^m$  to get global graph representation. (2) A clustering algorithm is applied on obtained embedding set to get  $K$  groups. Clustering centers of these groups are set to be anchors, annotated as  $\{\mathbf{h}^{l+1,k}\}_{k=1}^K$ . In experiments, we adopt DBSCAN [8] and tune its hyper-parameters to get around 20 groups. (3) At  $l$ -th layer,  $\mathbf{h}_v^{l+1}$  is represented in terms of relative distances to those  $K$  anchors, as  $\mathbf{s}_v^l \in \mathbb{R}^{1 \times K}$  with the  $k$ -th element calculated as  $\mathbf{s}_{v,k}^l = \|\mathbf{h}_v^{l+1} - \mathbf{h}_v^{l+1,k}\|_2$ . The alignment loss can be computed as:  $\mathcal{L}_{align}(f(\mathcal{G}), f(\mathcal{G}')) = \sum_l \sum_{v \in \mathcal{V}'} \|\mathbf{s}_v^l - \hat{\mathbf{s}}_v^l\|_2^2$ .

This alignment loss is used as an auxiliary task incorporated into MMI-based framework in Eq. 2 to get faithful explanation as:

$$\begin{aligned} & \min_{\mathcal{G}'} H_C(\hat{Y}, P(\hat{Y}' \mid \mathcal{G}')) + \lambda \cdot \mathcal{L}_{Align}, \\ & \text{s.t. } \mathcal{G}' \sim \mathcal{P}(\mathcal{G}, \mathbf{M}_A, \mathbf{M}_F), \quad \mathcal{R}(\mathbf{M}_F, \mathbf{M}_A) \leq c \end{aligned} \quad (5)$$

where  $\lambda$  controls the balance between prediction preservation and embedding alignment. Note that  $\mathcal{L}_{Align}$  is flexible to be incorporated into various existing explanation methods.

## 5 Analysis

From previous discussions, it is shown that  $\mathcal{G}'$  obtained via Eq. 1 cannot be safely used as explanations. We can summarize one main drawback of existing GNN explanation methods lies in the inductive bias: same outcomes do not guarantee the same causes, leaving existing approaches vulnerable towards spurious explanations. An illustration is given in Fig. 2(b). Objective proposed in Eq.( 1) optimizes the mutual information between explanation candidate  $\mathcal{G}'$  and  $\hat{Y}$ , corresponding to maximize the overlapping between  $H(\mathcal{G}')$  and  $H(\hat{Y})$  in Fig. 2(b), or region  $S_1 \cup S_2$  in Fig. 2(c). Here,  $H$  denotes information entropy. However, this learning target cannot prevent the danger of generating spurious explanations. Provided  $\mathcal{G}'$  may fall into the region  $S_2$ , which cannot faithfully represent graph  $\mathcal{G}$ . Instead, a more sensible objective should be maximizing region  $S_1$  in Fig. 2(c). The intuition behind this is that in the search input space that causes the same outcome, identified  $\mathcal{G}'$  should account for both representative and discriminative parts of original  $\mathcal{G}$ , in order to prevent spurious explanations that produce the same outcomes due to different causes. Concretely, this new explanation objective can be formalized as:

$$\begin{aligned} & \min_{\mathcal{G}'} -I(\mathcal{G}, \mathcal{G}', \hat{Y}), \\ \text{s.t. } & \mathcal{G}' \sim \mathcal{P}(\mathcal{G}, \mathbf{M}_A, \mathbf{M}_F) \quad \mathcal{R}(\mathbf{M}_F, \mathbf{M}_A) \leq c \end{aligned} \quad (6)$$

With some relaxations, it can be shown that our proposed method is in fact optimizing this new objective in Eq. 6. For the detailed derivation, please refer to Appendix. A

## 6 Experiment

In this section, we conduct a set of experiments to evaluate the benefits of proposed auxiliary task in providing instance-level post-hoc explanations. Experiments are conducted on 5 datasets, and obtained explanations are evaluated w.r.t both faithfulness and consistency.

### 6.1 Datasets

We conduct experiments on five publicly available benchmark datasets for explainability of GNNs, with statistics summarized in Table 1. BA-Shapes and Tree-Grid are node classification dataset introduced in [33], constructed by attaching ‘house’ or ‘grid’ motifs to base graphs (BA network or balanced binary tree). Nodes in the base graph are labeled as 0 and those in the motifs are labeled based on relative positions. Explanations are conducted on attached nodes of motifs, with edges inside

Table 1: Statistics of datasets

		BA-Shapes	Tree-Grid	Infection	Mutag	SST-5
Level	Node	Node	Node	Graph	Graph	
Graphs	1	1	1	4, 337	11, 855	
Avg.Nodes	700	1, 231	1, 000	30.3	19.8	
Avg.Edges	4, 110	3, 410	4, 001	61.5	18.8	
Labels	4	2	5	2	5	

the motif as ground-truth. Infection [9] is an ER graph with 5% of nodes labeled as infected. Other nodes are labeled based on their shortest distances to those infected ones, and labels larger than 4 are clipped. Nodes with multiple shortest paths are neglected, to guarantee that ground-truth explanation is unique. In Mutag [33], each graph corresponds to a molecule with nodes for atoms and edges for chemical bonds. Molecules are labeled with consideration of their chemical properties, and discriminative chemical groups are identified with prior domain knowledge [16]. Graph-SST5 [35] is constructed from text data, with labels from sentiment analysis. Each node represents a word and edges denote word dependencies. In this dataset, there is no ground-truth explanation provided, and heuristic metrics are adopted for evaluation.

### 6.2 Configurations

**Evaluation Metric** To evaluate *faithfulness* of different methods, we adopt two metrics: (1) AUROC score on edge importance and (2) Fidelity of explanations. On benchmarks with oracle explanations available, we can compute the AUROC score on identified edges as the well-trained target GNN

should follow those predefined explanations. On datasets without ground-truth explanations, we evaluate explanation quality with fidelity measurement following [35]. Concretely, we observe prediction changes by sequentially removing edges following assigned importance weight, and faster performance drop represents stronger fidelity.

To evaluate *consistency* of explanations, we randomly test each method 5 times, and report average structural hamming distance (SHD) [25] among obtained explanations. A smaller SHD score indicates stronger consistency across random running of the same method.

**Baseline** We select a group of representative and state-of-the-art instance-level post-hoc GNN explanation methods as the baselines, including (1) GRAD [16]: A gradient-based method, which assigns importance weights to edges based on back-propagated gradients; (2) ATT [16]: Utilizing average attention weights inside self-attention layers to distinguish important edges; (3) GNNExplainer [33]: A perturbation-based method which learns an importance matrix separately for every instance; (4) PGExplainer [16]: A parameterized explainer that learns a GNN to predict important edges for each graph; (5) Gem [15]: Similar to PGExplainer but from the causal view, learns edge importance based on estimated individual causal effect; (6) RG-Explainer [23]: A RL-enhanced explainer for GNN, constructs an explanatory subgraph by sequentially adding nodes with an RL agent.

**Settings** Following existing works [16], we train a three-layer GCN [14] on each dataset as the target model to be explained. All explainers are trained using ADAM optimizer with weight decay set to  $5e-4$ . For GNNExplainer, learning rate is initialized to 0.01 with learning epoch being 100. For PGExplainer, learning rate is initialized to 0.003 and training epoch is set as 30. Hyper-parameter  $\lambda$ , which controls the weight of  $\mathcal{L}_{align}$ , is tuned via grid search on each dataset. For our method, both variants of embedding alignment are implemented, and we incorporate them into two representative GNN explanation frameworks, i.e., GNNExplainer [33] and PGExplainer [16].

### 6.3 Explanation Faithfulness

#### 6.3.1 AUROC on Edges

In this subsection, AUROC scores of different methods are reported by comparing assigned edge importance weight with ground-truth explanations. For baseline methods GRAD, ATT, Gem, and RG-Explainer, their performances reported in their original papers are presented. GNNExplainer and PGExplainer are re-implemented, upon which two alignment strategies are instantiated and tested. Each experiment is randomly conducted 5 times, and we summarize the average performance in Table 2. A higher AUROC score indicates more accurate explanations. From the results, we can make the following observations: (1) Across all four datasets, with both GNNExplainer or PGExplainer as the base method, incorporating embedding alignment can improve the quality of obtained explanations; (2) In most cases, anchor-based alignment demonstrates stronger improvements, which shows the benefits of utilizing global distribution information; (3) On more complex datasets like Mutag, the benefit of introducing embedding alignment is clearer. This result indicates that the problem of spurious explanations is severer with increased dataset complexity.

Table 2: Explanation Faithfulness in terms of AUC on Edges

	BA-Shapes	Tree-Grid	Infection	Mutag
GRAD	88.2	61.2	74.0	78.3
ATT	81.5	66.7	–	76.5
Gem	97.1	–	–	83.4
RG-Explainer	98.5	92.7	–	87.3
GNNExplainer	$93.1 \pm 1.8$	$86.2 \pm 2.2$	$92.2 \pm 1.1$	$74.9 \pm 1.9$
+ Align_Emb	$95.3 \pm 1.4$	$91.2 \pm 2.3$	$93.0 \pm 1.0$	$76.3 \pm 1.7$
+ Align_Anchor	$97.1 \pm 1.3$	$92.4 \pm 1.9$	$93.1 \pm 0.8$	$78.9 \pm 1.6$
PGExplainer	$96.9 \pm 0.7$	$92.7 \pm 1.5$	$89.6 \pm 0.6$	$83.7 \pm 1.2$
+ Align_Emb	$97.2 \pm 0.7$	$95.8 \pm 0.9$	$90.5 \pm 0.7$	$92.8 \pm 1.1$
+ Align_Anchor	$98.7 \pm 0.5$	$94.7 \pm 1.2$	$91.6 \pm 0.6$	$94.5 \pm 0.8$

#### 6.3.2 Explanation Fidelity

In addition to comparing to ground-truths explanations, we also evaluate the obtained explanations in terms of fidelity. Specifically, we sequentially removing edges from the graph by following importance weight learned by the explanation model and test the classification performance. Generally, the removal of really important edges would significantly degrade the classification performance. Thus,

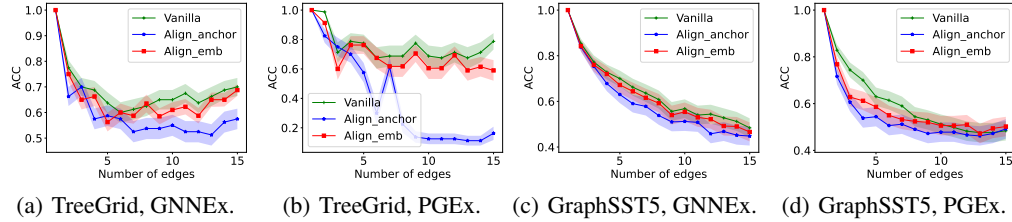


Figure 3: Fidelity curve on Tree-Grid and Graph-SST5, with our method tested on both GNNExplainer and PGExplainer. Faster drop indicates stronger truthfulness of obtained explanations.

a faster performance drop represents stronger fidelity. We conduct experiments on Tree-Grid and Graph-SST5. Each experiment is conducted 3 times and we report the obtained fidelity curve in Fig. 3. From the figure, we can observe that when proposed embedding alignment is incorporated, the classification accuracy from edge removal drops much faster, which shows that the proposed embedding alignment can help to identify more important edges used by GNN for classification, hence providing better explanations. Furthermore, anchor-based alignment is shown to be more effective, validating advantages in distribution-aware alignment.

#### 6.4 Explanation Consistency

One problem of spurious explanation is that multiple rounds of random running could lead to different results, violating the *consistency* property of explanations. In this section, we examine consistency of each method by randomly testing them for 5 times. Specifically, SHD distance among explanatory edges with top- $k$  importance weights identified each time is computed. We select GNNExplainer and PGExplainer as the backbone, and the averaged results on Tree-Grid and Mutag are reported in Table 3. Larger distances indicate inconsistent explanations.

From the table, it can be observed that existing method following Eq. 1 suffer from the consistency problem. For example, average SHD distance on top-6 edges is 4.39 for GNNExplainer. Introducing the auxiliary task of aligning embeddings can significantly improve explainers in terms of this criterion. After incorporating anchor-based alignment, SHD distance of top-6 edges drops from 4.39 to 2.21 for GNNExplainer, from 1.38 to 0.13 for PGExplainer, which validates effectiveness of our proposal in obtaining consistent explanations.

Table 3: Consistency of Top-1 to Top-6 identified explanatory edges in terms of SHD distance.

	TreeGrid						Mutag					
	1	2	3	4	5	6	1	2	3	4	5	6
GNNExplainer	0.86	1.85	2.48	3.14	3.77	4.39	1.12	1.74	2.65	3.40	4.05	4.78
+Align_Emb	0.77	1.23	1.28	0.96	1.81	2.72	1.05	1.61	2.33	3.15	3.77	4.12
+Align_Anchor	0.72	1.06	0.99	0.53	1.52	2.21	1.06	1.59	2.17	3.06	3.54	3.95
PGExplainer	0.74	1.23	0.76	0.46	0.78	1.38	0.91	1.53	2.10	2.57	3.05	3.42
+Align_Emb	0.11	0.15	0.13	0.11	0.24	0.19	0.55	0.96	1.13	1.31	1.79	2.04
+Align_Anchor	0.07	0.12	0.13	0.16	0.21	0.13	0.51	0.90	1.05	1.27	1.62	1.86

These results verify the effectiveness of our method in obtaining more faithful and consistent explanations. More experiments are presented in Appendix B due to space limitation.

## 7 Related Work

### 7.1 Graph Neural Networks

Graph neural networks (GNNs) are developing rapidly in recent years, with the increasing need for learning on relational data structures [10, 5, 40]. Generally, existing GNNs can be categorized into two categories, i.e., spectral-based approaches [4, 24, 14] based on graph signal processing

theory, and spatial-based approaches [7, 1, 31] relying upon neighborhood aggregation. Despite their differences, most GNN variants can be summarized with the message-passing framework, which is composed of pattern extraction and interaction modeling within each layer [11]. Specifically, GNNs model messages from node representations. These messages are then propagated with various message-passing mechanisms to refine node representations, which are then utilized for downstream tasks, such as node/graph classification [12] and link prediction [37, 40]. Despite their success in network representation learning, GNNs are uninterpretable black box models. It is challenging to understand their behaviors even if the adopted message passing mechanism and parameters are given. Besides, unlike traditional deep neural networks where instances are identically and independently distributed, GNNs consider node features and graph topology jointly, making the interpretability problem more challenging to handle.

## 7.2 GNN Interpretation Methods

Many efforts have been taken to interpret GNN models and provide explanations for their predictions [28]. Existing methods can be generally grouped into two categories: (1) Instance-level explanation [33, 22, 29], which provides explanations on the prediction for each instance by identifying important substructures; and (2) Model-level explanation [3, 38, 34], which aims to understand global decision rules captured by the target GNN. For each group, existing methods can be further categorized as (1) self-explainable GNNs [38, 6], where the GNN can simultaneously give prediction and explanations on the prediction; and (2) post-hoc explanations [33, 16, 36], which adopt another model or strategy to provide explanations of a target GNN. As post-hoc explanations are model-agnostic, i.e., can be applied for various GNNs, in this work, we focus on post-hoc instance-level explanations [33], i.e., given a trained GNN model, identify instance-wise critical substructures for each input to explain the prediction.

Existing methods have explored a variety of strategies for post-hoc instance-level explanations, e.g., based on signals from gradients [19, 3], perturbed predictions [33, 16, 36, 23], decomposition [3, 21], etc. Most methods adopt the second strategy, i.e., learning a perturbation mask to maximally mask out non-important edges so as to identify important substructure that can preserve original predictions [35]. The identified important substructure is used as explanation for the prediction. For example, GNNExplainer [33] employs two soft masks on node attributes and edges, respectively, which are learned end-to-end under the maximizing mutual information (MMI) framework. SubgraphX [36] employs Monte Carlo Tree Search (MCTS) to find connected subgraphs that preserve predictions as explanation. Similar to ours, RCEExplainer [2] also seeks for more faithful explanations by examining inference process of the target GNN. However, it requires discovering submodular cover of classification boundaries and involves complex pro-processing, which is difficult to work in together with other explanation strategies.

Despite progress in interpreting GNNs, most of these methods discover critical substructures merely upon the change of outputs given perturbed inputs, and are heavily affected by spurious correlations caused by confounding factors in the environment. On the other hand, by aligning intermediate embeddings in GNNs, our method alleviates effects of spurious correlations on interpreting GNNs, leading to faithful and consistent explanations.

## 8 Conclusion

In this work, we study a novel problem of obtaining faithful and consistent explanations for GNNs, which is largely neglected by existing MMI-based explanation framework. With close analysis on inference of GNNs, we propose a simple yet effective approach by aligning internal embeddings of the raw graph and its candidate explainable subgraph. Concretely, two aligners are designed based on absolute distance and global distributions respectively, which can be incorporated into existing methods like GNNExplainer and PGExplainer with no effort. Experiments validate the effectiveness of our proposal, and further analysis shows that it is more faithful in design, optimizing a new explanation objective.

In the future, works can be done seeking more robust explanations. Similar graphs should have similar explanations. Furthermore, increased robustness indicates stronger generality, and could provide better class-level interpretation at the same time.

## References

- [1] James Atwood and Don Towsley. 2016. Diffusion-convolutional neural networks. In *Advances in neural information processing systems*. 1993–2001.
- [2] Mohit Bajaj, Lingyang Chu, Zi Yu Xue, Jian Pei, Lanjun Wang, Peter Cho-Ho Lam, and Yong Zhang. 2021. Robust counterfactual explanations on graph neural networks. *Advances in Neural Information Processing Systems* 34 (2021).
- [3] Federico Baldassarre and Hossein Azizpour. 2019. Explainability techniques for graph convolutional networks. *arXiv preprint arXiv:1905.13686* (2019).
- [4] Joan Bruna, Wojciech Zaremba, Arthur Szlam, and Yann LeCun. 2013. Spectral networks and locally connected networks on graphs. *arXiv preprint arXiv:1312.6203* (2013).
- [5] Enyan Dai, Wei Jin, Hui Liu, and Suhang Wang. 2022. Towards Robust Graph Neural Networks for Noisy Graphs with Sparse Labels. *arXiv preprint arXiv:2201.00232* (2022).
- [6] Enyan Dai and Suhang Wang. 2021. Towards Self-Explainable Graph Neural Network. In *Proceedings of the 30th ACM International Conference on Information & Knowledge Management*. 302–311.
- [7] David K Duvenaud, Dougal Maclaurin, Jorge Iparraguirre, Rafael Bombarell, Timothy Hirzel, Alán Aspuru-Guzik, and Ryan P Adams. 2015. Convolutional networks on graphs for learning molecular fingerprints. In *Advances in neural information processing systems*. 2224–2232.
- [8] Martin Ester, Hans-Peter Kriegel, Jörg Sander, Xiaowei Xu, et al. 1996. A density-based algorithm for discovering clusters in large spatial databases with noise.. In *kdd*, Vol. 96. 226–231.
- [9] Lukas Faber, Amin K. Moghaddam, and Roger Wattenhofer. 2021. When Comparing to Ground Truth is Wrong: On Evaluating GNN Explanation Methods. In *Proceedings of the 27th ACM SIGKDD Conference on Knowledge Discovery & Data Mining*. 332–341.
- [10] Wenqi Fan, Y. Ma, Qing Li, Yuan He, Y. Zhao, Jiliang Tang, and D. Yin. 2019. Graph Neural Networks for Social Recommendation. *The World Wide Web Conference* (2019).
- [11] Justin Gilmer, Samuel S Schoenholz, Patrick F Riley, Oriol Vinyals, and George E Dahl. 2017. Neural Message Passing for Quantum Chemistry. In *ICML*.
- [12] Will Hamilton, Zhitao Ying, and Jure Leskovec. 2017. Inductive representation learning on large graphs. *Advances in neural information processing systems* 30 (2017).
- [13] Qiang Huang, Makoto Yamada, Yuan Tian, Dinesh Singh, Dawei Yin, and Yi Chang. 2020. Graphlime: Local interpretable model explanations for graph neural networks. *arXiv preprint arXiv:2001.06216* (2020).
- [14] Thomas N Kipf and Max Welling. 2016. Semi-supervised classification with graph convolutional networks. *arXiv preprint arXiv:1609.02907* (2016).
- [15] Wanyu Lin, Hao Lan, and Baochun Li. 2021. Generative causal explanations for graph neural networks. In *International Conference on Machine Learning*. PMLR, 6666–6679.
- [16] Dongsheng Luo, Wei Cheng, Dongkuan Xu, Wenchao Yu, Bo Zong, Haifeng Chen, and Xiang Zhang. 2020. Parameterized explainer for graph neural network. *Advances in neural information processing systems* 33 (2020), 19620–19631.
- [17] Elman Mansimov, O. Mahmood, Seokho Kang, and Kyunghyun Cho. 2019. Molecular Geometry Prediction using a Deep Generative Graph Neural Network. *Scientific Reports* 9 (2019).
- [18] Meike Nauta, Jan Trienes, Shreyasi Pathak, Elisa Nguyen, Michelle Peters, Yasmin Schmitt, Jörg Schlätterer, Maurice van Keulen, and Christin Seifert. 2022. From Anecdotal Evidence to Quantitative Evaluation Methods: A Systematic Review on Evaluating Explainable AI. *arXiv preprint arXiv:2201.08164* (2022).

[19] Phillip E Pope, Soheil Kolouri, Mohammad Rostami, Charles E Martin, and Heiko Hoffmann. 2019. Explainability methods for graph convolutional neural networks. In *Proceedings of the IEEE/CVF Conference on Computer Vision and Pattern Recognition*. 10772–10781.

[20] Jiahua Rao, Shuangjia Zheng, and Yuedong Yang. 2021. Quantitative Evaluation of Explainable Graph Neural Networks for Molecular Property Prediction. *arXiv preprint arXiv:2107.04119* (2021).

[21] Thomas Schnake, Oliver Eberle, Jonas Lederer, Shinichi Nakajima, Kristof T Schütt, Klaus-Robert Müller, and Grégoire Montavon. 2020. Higher-order explanations of graph neural networks via relevant walks. *arXiv preprint arXiv:2006.03589* (2020).

[22] Patrick Schwab and Walter Karlen. 2019. Cxplain: Causal explanations for model interpretation under uncertainty. *Advances in Neural Information Processing Systems* 32 (2019).

[23] Caihua Shan, Yifei Shen, Yao Zhang, Xiang Li, and Dongsheng Li. 2021. Reinforcement Learning Enhanced Explainer for Graph Neural Networks. *Advances in Neural Information Processing Systems* 34 (2021).

[24] S. Tang, Bo Li, and Haijun Yu. 2019. ChebNet: Efficient and Stable Constructions of Deep Neural Networks with Rectified Power Units using Chebyshev Approximations. *ArXiv abs/1911.05467* (2019).

[25] Ioannis Tsamardinos, Laura E Brown, and Constantin F Aliferis. 2006. The max-min hill-climbing Bayesian network structure learning algorithm. *Machine learning* 65, 1 (2006), 31–78.

[26] Michel Verleysen and Damien François. 2005. The curse of dimensionality in data mining and time series prediction. In *International work-conference on artificial neural networks*. Springer, 758–770.

[27] Minh N Vu and My T Thai. 2020. Pgm-explainer: Probabilistic graphical model explanations for graph neural networks. *arXiv preprint arXiv:2010.05788* (2020).

[28] Xiang Wang, Yingxin Wu, An Zhang, Xiangnan He, and Tat-seng Chua. 2020. Causal Screening to Interpret Graph Neural Networks. (2020).

[29] Xiang Wang, Yingxin Wu, An Zhang, Xiangnan He, and Tat-Seng Chua. 2021. Towards Multi-Grained Explainability for Graph Neural Networks. *Advances in Neural Information Processing Systems* 34 (2021).

[30] Ying-Xin Wu, Xiang Wang, An Zhang, Xiangnan He, and Tat-Seng Chua. 2022. Discovering Invariant Rationales for Graph Neural Networks. *arXiv preprint arXiv:2201.12872* (2022).

[31] Teng Xiao, Zhengyu Chen, Donglin Wang, and Suhang Wang. 2021. Learning how to propagate messages in graph neural networks. In *Proceedings of the 27th ACM SIGKDD Conference on Knowledge Discovery & Data Mining*. 1894–1903.

[32] Keyulu Xu, Weihua Hu, Jure Leskovec, and Stefanie Jegelka. 2018. How powerful are graph neural networks? *arXiv preprint arXiv:1810.00826* (2018).

[33] Rex Ying, Dylan Bourgeois, Jiaxuan You, Marinka Zitnik, and Jure Leskovec. 2019. Gnnexplainer: Generating explanations for graph neural networks. *Advances in neural information processing systems* 32 (2019), 9240.

[34] Hao Yuan, Jiliang Tang, Xia Hu, and Shuiwang Ji. 2020. Xgnn: Towards model-level explanations of graph neural networks. In *Proceedings of the 26th ACM SIGKDD International Conference on Knowledge Discovery & Data Mining*. 430–438.

[35] Hao Yuan, Haiyang Yu, Shurui Gui, and Shuiwang Ji. 2020. Explainability in graph neural networks: A taxonomic survey. *arXiv preprint arXiv:2012.15445* (2020).

[36] Hao Yuan, Haiyang Yu, Jie Wang, Kang Li, and Shuiwang Ji. 2021. On explainability of graph neural networks via subgraph explorations. In *International Conference on Machine Learning*. PMLR, 12241–12252.

- [37] Muhan Zhang and Yixin Chen. 2018. Link prediction based on graph neural networks. *Advances in neural information processing systems* 31 (2018).
- [38] Zaixi Zhang, Qi Liu, Hao Wang, Chengqiang Lu, and Cheekong Lee. 2021. ProtGNN: Towards Self-Explaining Graph Neural Networks. *arXiv preprint arXiv:2112.00911* (2021).
- [39] Tianxiang Zhao, Xianfeng Tang, Xiang Zhang, and Suhang Wang. 2020. Semi-Supervised Graph-to-Graph Translation. In *Proceedings of the 29th ACM International Conference on Information & Knowledge Management*. 1863–1872.
- [40] Tianxiang Zhao, Xiang Zhang, and Suhang Wang. 2021. GraphSMOTE: Imbalanced Node Classification on Graphs with Graph Neural Networks. In *Proceedings of the Fourteenth ACM International Conference on Web Search and Data Mining*.

## A Method Analysis

$I(\mathcal{G}, \mathcal{G}', \hat{Y})$  is intractable as latent generation mechanism of  $\mathcal{G}$  is unknown. In this part, we expand this objective, connect it to Equation 5, and construct its proxy optimizable form:

$$\begin{aligned}
I(\mathcal{G}, \mathcal{G}', \hat{Y}) &= \sum_{y \sim \hat{Y}} \sum_{\mathcal{G}} \sum_{\mathcal{G}'} P(\mathcal{G}, \mathcal{G}', y) \cdot \log \frac{P(\mathcal{G}', y) P(\mathcal{G}, \mathcal{G}') P(\mathcal{G}, y)}{P(\mathcal{G}, \mathcal{G}', y) P(\mathcal{G}) P(\mathcal{G}') P(y)} \\
&= \sum_{y \sim \hat{Y}} \sum_{\mathcal{G}} \sum_{\mathcal{G}'} P(\mathcal{G}, \mathcal{G}', y) \cdot \log \left[ \frac{P(\mathcal{G}', y)}{P(\mathcal{G}') P(y)} \cdot \frac{P(\mathcal{G}, \mathcal{G}')}{P(\mathcal{G}) P(\mathcal{G}')} \cdot \frac{P(\mathcal{G}, y)}{P(\mathcal{G}, y | \mathcal{G}')} \right] \\
&= \sum_{y \sim \hat{Y}} \sum_{\mathcal{G}'} P(\mathcal{G}', y) \cdot \log \frac{P(\mathcal{G}', y)}{P(\mathcal{G}') P(y)} + \sum_{\mathcal{G}} \sum_{\mathcal{G}'} P(\mathcal{G}, \mathcal{G}') \cdot \log \frac{P(\mathcal{G}, \mathcal{G}')}{P(\mathcal{G}) P(\mathcal{G}')} \\
&\quad - \sum_{\mathcal{G}'} \sum_{y \sim \hat{Y}} \sum_{\mathcal{G}} P(\mathcal{G}, y, \mathcal{G}') \cdot \log \frac{P(\mathcal{G}, y, \mathcal{G}')}{P(\mathcal{G}, y) P(\mathcal{G}')} \\
&= I(\mathcal{G}', \hat{Y}) + I(\mathcal{G}, \mathcal{G}') - \sum_{y \sim \hat{Y}} \sum_{\mathcal{G}} P(\mathcal{G}, y) \sum_{\mathcal{G}'} P(\mathcal{G}' | \mathcal{G}, y) \cdot \log P(\mathcal{G}' | \mathcal{G}, y) \\
&\quad + \sum_{\mathcal{G}'} \sum_{y \sim \hat{Y}} \sum_{\mathcal{G}} P(\mathcal{G}, y, \mathcal{G}') \cdot \log P(\mathcal{G}') \\
&= I(\mathcal{G}', \hat{Y}) + I(\mathcal{G}, \mathcal{G}') + H(\mathcal{G}' | \mathcal{G}, \hat{Y}) - H(\mathcal{G}').
\end{aligned}$$

Since both  $H(\mathcal{G}' | \mathcal{G}, \hat{Y})$  and  $H(\mathcal{G}')$  depicts entropy of explanation  $\mathcal{G}'$  and are closely related to perturbation budgets, we can neglect these two terms and get a surrogate optimization objective for  $\max_{\mathcal{G}'} I(\mathcal{G}, \mathcal{G}', \hat{Y})$  as  $\max_{\mathcal{G}'} I(\hat{Y}, \mathcal{G}') + I(\mathcal{G}', \mathcal{G})$ .

With the observation that  $\max_{\mathcal{G}'} I(\mathcal{G}, \mathcal{G}', \hat{Y})$  can be approximated by  $\max_{\mathcal{G}'} I(\hat{Y}, \mathcal{G}') + I(\mathcal{G}', \mathcal{G})$ , it can be further noted that  $\max_{\mathcal{G}'} I(\hat{Y}, \mathcal{G}')$  is the same as Eq.( 1). Following [33], We relax it as  $\min_{\mathcal{G}'} H_C(\hat{Y}, \hat{Y}' | \mathcal{G}')$ , optimizing  $\mathcal{G}'$  to preserve original prediction outputs. The second term,  $\max_{\mathcal{G}'} I(\mathcal{G}', \mathcal{G})$ , corresponds to maximizing consistency between  $\mathcal{G}'$  and  $\mathcal{G}$ . Although the graph generation process is latent, with the safe assumption that embedding  $\mathbf{E}_{\mathcal{G}}$  extracted by  $f$  is representative of  $\mathcal{G}$ , we can construct a proxy objective  $\max_{\mathcal{G}'} I(\mathbf{E}_{\mathcal{G}'}, \mathbf{E}_{\mathcal{G}})$ , improving the consistency in the embedding space. In this work, we optimize this objective by aligning their representations, either optimizing a simplified distance metric or conducting distribution-aware alignment.

## B More Experiments

### B.1 Ability in Avoiding Spurious Explanations

Existing graph explanation benchmarks are usually designed to be less ambiguous, containing only one oracle cause of labels, and identified explanatory substructures are evaluated via comparing with the ground-truth explanation. However, this result could be misleading, as faithfulness of explanation methods in more complex scenarios is left untested. Real-world datasets are usually rich in spurious patterns and a trained GNN could contain diverse biases, setting a tighter requirement on explanation methods. Thus, to evaluate if our framework can alleviate the spurious explanation issue, we create a new graph-classification dataset: MixMotif, which enables us to train a biased GNN model, and test whether explanation methods can successfully expose this bias.

Specifically, inspired by [30], we design three types of base graphs, i.e., Tree, Ladder, Wheel, and three types of motifs, i.e., Cycle, House, and Grid. With a mix ratio  $\gamma$ , motifs are preferably attached to base graphs. For example, Cycle is attached to Tree with probability  $\frac{2}{3}\gamma + \frac{1}{3}$ , and to others with probability  $\frac{1-\gamma}{3}$ . So are the cases for House to Ladder and Grid to Wheel. Labels of obtained graphs are set as type of the motif. When  $\gamma$  is set to 0, each motif has the same probability being attached to the three base graphs. In other words, there's no bias on which type of base graph to attach for each type of motif. Thus, we consider the dataset with  $\gamma = 0$  is clean or bias-free. We would expect GNN trained on data with  $\gamma = 0$  to focus on the motif structure for motif classification. However, when  $\gamma$  becomes larger, the spurious correlation between base graph and the label would exist, i.e., a GNN might utilize the base graph structure for motif classification instead of relying on the motif

structure. For each setting, the created dataset contains 3,000 graphs, and train:evaluation:test are split as 5 : 2 : 3.

In this experiment, we set  $\gamma$  to 0 and 0.7 separately, and train GNN  $f_0$  and  $f_{0.7}$  for each setting. Two models are tested in graph classification performance. Then, explanation methods are applied to and fine-tuned on  $f_0$ . Following that, these explanation methods are applied to explain  $f_{0.7}$  using found hyper-parameters. Results are summarized in Table 4.

From Table 4, we can observe that (1)  $f_0$  achieves almost perfect graph classification performance during testing. This high accuracy indicates that it captures the genuine pattern, relying on motifs to make predictions. Looking at explanation results, it is shown that our proposal offers more faithful explanations, achieving higher AUROC on motifs. (2)  $f_{0.7}$  fails to predict well with  $\gamma = 0$ , showing that there are biases in it and it no longer depends solely on the motif structure for prediction. Although ground-truth explanations are unknown in this case, a successful explanation should expose this bias. However, PGExplainer would produce similar explanations as the clean model, still highly in accord with motif structures. Instead, for explanations produced by embedding alignment, AUROC score would drop from 0.795 to 0.266, exposing the change in prediction rationales, hence able to expose biases. (3) In summary, our proposal can provide more faithful explanations for both clean and mixed settings, while PGExplainer would suffer from spurious explanations and fail to faithfully explain GNN’s predictions, especially in the existence of biases.

## B.2 Ablation Study

In this part, we conduct ablation study by varying hyper-parameter  $\lambda$ , which controls the weight of our proposed embedding alignment task. To keep simplicity, all other configurations are kept unchanged, and  $\lambda$  varies within the scale  $\{1e-3, 1e-2, 1e-1, 1, 10, 1e2, 1e3\}$ . Experiments are randomly conducted 3 times on dataset Tree-Grid and Mutag, and PGExplainer is adopted as the base method. Results are visualized in Figure 4. From the figure, we can observe that increasing  $\lambda$  has a positive effect at first, and further increase would result in a performance drop. Besides, anchor-based alignment usually requires a smaller weight to show improvements.

Table 4: Performance on MixMotif. Two GNNs are trained with different  $\gamma$ . We check their performance in graph classification, then compare obtained explanations with the motif.

		$\gamma$ in Training		
Classification		0	0.7	
$\gamma$ in test	0	0.982	0.765	
	0.7	0.978	0.994	
Explanation	PGExplainer	+Align	PGExplainer	+Align
AUROC on Motif	0.711	<b>0.795</b> (Higher is better)	0.748	<b>0.266</b> (Lower is better)

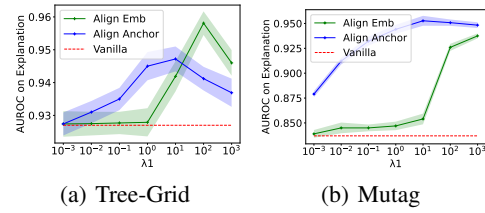


Figure 4: Sensitivity of PGExplainer towards weight of embedding alignment loss.